Research

Cite this article: O'Malley AJ, García Sakai V, Dimitratos N, Jones W, Catlow CRA, Parker SF. 2020 Octane isomer dynamics in H-ZSM-5 as a function of Si/Al ratio: a quasi-elastic neutron scattering study.

One contribution of 14 to a discussion meeting issue 'Science to enable the circular economy'.

Subject Areas:
materials science, inorganic chemistry, physical chemistry

Keywords:
fluid catalytic cracking, zeolite, neutron, quasi-elastic neutron scattering, molecular mobility

Author for correspondence:
Alexander J. O'Malley e-mail:
a.o'malley@bath.ac.uk

Octane isomer dynamics in H-ZSM-5 as a function of Si/Al ratio: a quasi-elastic neutron scattering study

Alexander J. O'Malley[1,2], Victoria García Sakai[3], Nikolaos Dimitratos[4], Wilm Jones[2,6], C. Richard A. Catlow[2,5,6] and Stewart F. Parker[2,3]

[1]Centre for Sustainable and Circular Technologies, Department of Chemistry, University of Bath, Claverton Down, Bath BA2 7AY, UK [2]UK Catalysis Hub, Research Complex at Harwell, Science and Technology Facilities Council Rutherford Appleton Laboratory, Harwell Science and Innovation Campus, Oxon OX11 0QX, UK

[3]ISIS Pulsed Neutron and Muon Facility, Science and Technology Facilities Council Rutherford Appleton Laboratory, Harwell Science and Innovation Campus, Oxon OX11 0QX, UK

[4]Dipartimento di Chimica Industriale e dei Materiali, ALMA MATER STUDIORUM, Università di Bologna, Viale Risorgimento 4, 40136 Bologna, Italy

[5]Cardiff Catalysis Department, School of Chemistry, Cardiff University, Cardiff, CF10 3AT, UK

[6]Department of Chemistry, University College London, 20 Gordon St., London WC1 HOAJ, UK

AJOM, 0000-0002-6221-4333; VGS, 0000-0001-6570-4218; ND, 0000-0002-6620-4335; SFP, 0000-0002-3228-2570

Dynamical behaviour of *n*-octane and 2,5-dimethylhexane in H-ZSM-5 zeolite catalysts of differing Si/Al ratios (15 and 140) was probed using quasi-elastic neutron scattering, to understand molecular shape and Brønsted acid site density effects on the behaviour of common species in the fluid catalytic cracking (FCC) process, where H-ZSM-5 is an additive catalyst. Between 300 and 400 K, *n*-octane displayed uniaxial rotation around its long axis. However, the population of mobile molecules was larger in H-ZSM-5(140), suggesting that the lower acid site concentration allows for more molecules to undergo rotation. The rotational diffusion coefficients

were higher in H-ZSM-5(140), reflecting this increase in freedom. 2,5-dimethylhexane showed qualitative differences in behaviour to *n*-octane, with no full molecule rotation, probably due to steric hindrance in the constrictive channels. However, methyl group rotation in the static 2,5-dimethylhexane molecules was observed, with lower mobile fractions in H-ZSM-5(15), suggesting that this rotation is less hindered when fewer Brønsted sites are present. This was
further illustrated by the lower activation barrier calculated for methyl rotation in H-ZSM-5(140). We highlight the significant immobilizing effect of isomeric branching in this important industrial catalyst and show how compositional changes of the zeolite can affect a range of dynamical behaviours of common FCC species upon adsorption.

This article is part of a discussion meeting issue ‘Science to enable the circular economy’.

1. Introduction

The behaviour of hydrocarbons in zeolite catalysts is of great interest to a number of applications relevant to the circular economy. One such application is the optimization/adaptation of processes such as fluid catalytic cracking (FCC) of crude oil fractions, to accommodate renewable feedstocks. FCC is one of the major conversion technologies in the petrochemical industry responsible for much of the world’s gasoline [1], where approximately 2300 metric tons of FCC catalyst are produced per day based, primarily, on zeolite Y [2] but also ZSM-5, to promote small hydrocarbon products such as propene [3]. The modification of this process to accommodate renewable feedstocks such as biomass [4,5] and even plastic waste [6], requires an in-depth knowledge of how the relevant hydrocarbon species behave in the catalyst micropores.

Of great interest is the effect of molecular shape and branching on the mobility of hydrocarbons, which is fundamental to the shape selectivity characteristics of zeolites [7,8]. These studies are difficult due to the most important processes taking place under confinement in the porous matrix of the zeolite. However, a significant amount of work, both theoretical and experimental, has been carried out studying the mobility of hydrocarbons in the MFI zeolite structure [9–16], the framework of H-ZSM-5, and increases in computational power have led to relatively inexpensive computational models of alkane dosed MFI systems that calculate diffusion coefficients close to those observed by experiment [17–19].

Techniques based on neutron spectroscopy are particularly powerful for studying not only structural and active site characteristics of the catalyst [20–23] but also the dynamical behaviour of hydrocarbons in microporous catalysts [24], where quasi-elastic neutron scattering (QENS) may probe dynamics on the timescale of rotational and translational diffusion [24]. Previous work has employed QENS to study *n*-alkanes in the MFI structure [25,26] typically yielding diffusion coefficients in the range of approximately 10^{-10} m^2 s^{-1} . Branched alkanes diffuse over an order of magnitude more slowly [27] and often require higher resolution techniques such as neutron spin echo to gain reliable measurements [19]. Recent work has shown some very revealing insights into localized behaviours, such as the rotation of 1-octene oligomers in the ZSM-5 straight channels [28], and it is clear that such localized motions can bring significant insight into the behaviour of important species as a function of molecular size and shape [29], composition (where the presence of counterions in the framework can significantly affect molecular mobility [25]) and even catalyst use [30].

To this end, we have employed quasi-elastic neutron scattering to probe the mobility of common FCC C_8 isomers *n*-octane and 2,5-dimethylhexane in H-ZSM-5, while varying the Si/Al ratio of the catalyst and thus the density of strongly adsorbing Brønsted acid sites. We show that the branching of 2,5-dimethylhexane in the 5.5 Å ZSM-5 micropores causes significant qualitative differences in dynamics compared to the straight chain analogue, and that the difference in Brønsted acid site concentration affects the quantitative aspects, such as the size of mobile fractions, and rates of motion observed for both species.

2. Experimental section

(a) Materials

The ZSM-5 samples used were commercial zeolite catalysts obtained from Zeolyst International with Si/Al ratio = 15 (CBV3024E) and 140 (CBV28014) referred to herein as H-ZSM-5(15) and H-ZSM-5(140), respectively. Their bulk crystallinity has been verified by powder X-ray diffraction in recent studies [31,32]. The samples arrived in their ammonium form and were calcined to achieve the catalytic proton form. This was carried out in air, heating at 1°C min^{-1} up to 150°C followed by 5°C min^{-1} to 500°C, where they were held for 4 h. The samples were then dried at 150°C for 4 h under flowing helium. After cooling, the alkanes were loaded by passing He carrier gas through a Dreschel bottle containing the alkane. The samples were loaded to approximately 1 molecule of alkane per unit cell, determined gravimetrically.

(b) Quasi-elastic neutron scattering experiments

QENS experiments were carried out using the time-of-flight backscattering neutron spectrometer OSIRIS [33] at the ISIS Pulsed Neutron and Muon Source (UK). The cells were placed in a top loading closed cycle refrigerator. Each sample was then cooled to a base temperature of 10 K and a resolution measurement was taken. The samples were then heated to 300, 360 and 400 K where the QENS spectra were measured. A pyrolytic graphite 002 analyser was used giving an energy resolution of 24.5 µeV with energy transfers measured in a window of ±0.55 meV; the detector coverage enabled measurements over a Q range of 0.2–1.75 $Å^{-1}$. A measurement was taken of the empty ZSM-5 samples and the signal was then subtracted from the signal of the sorbate loaded ZSM-5, so that the signal from the sorbate only, could be extracted. In this way any scattering from the aluminium container, which was very low in comparison with the zeolite, was also subtracted. No further corrections were necessary. All QENS spectra were fitted using the neutron scattering analysis software packages, DAVE [34] and MANTID [35].

3. Results and discussion

(a) *n*-octane dynamics

QENS spectra as a function of the momentum transfer vector Q at 300 K are shown in figure 1*a* and *b* for *n*-octane in H-ZSM-5(15) and (140), respectively. The spectra were fitted to a delta function convoluted with the resolution measurement taken at 10 K, a single Lorentzian function (which was enough to describe the data satisfactorily) and a flat background function.

The figures contain the data points, the total fit (black) and the quasi-elastic component of the spectra (red) given by the Lorentzian function.

The presence of a large elastic component in all the spectra suggests that either a large fraction of immobile molecules is present or localized motions such as rotations are taking place, or both. One may characterize the possible localized motions using the elastic incoherent structure factor (EISF) [36,37] which is given in equation (3.1), and is the proportion of the total scattered intensity which is elastic.

$$A_0(Q) = \frac{I_{\text{elastic}}(Q)}{I\text{elastic}(Q) + I\text{QENS}(Q)}. \tag{3.1}$$

The experimental EISF for *n*-octane is shown in figure 2, along with models for localized octane motion as outlined in our previous work [28]. These include the Volino and Dianoux model of diffusion confined to sphere, with a radius (r_{conf}) matching that of a ZSM-5 channel, where the EISF is given by equation (3.2).

$$A_0(Q) = \left[\frac{3j_1(Qr_{\text{conf}})}{Qr_{\text{conf}}}\right]^2, \tag{3.2}$$

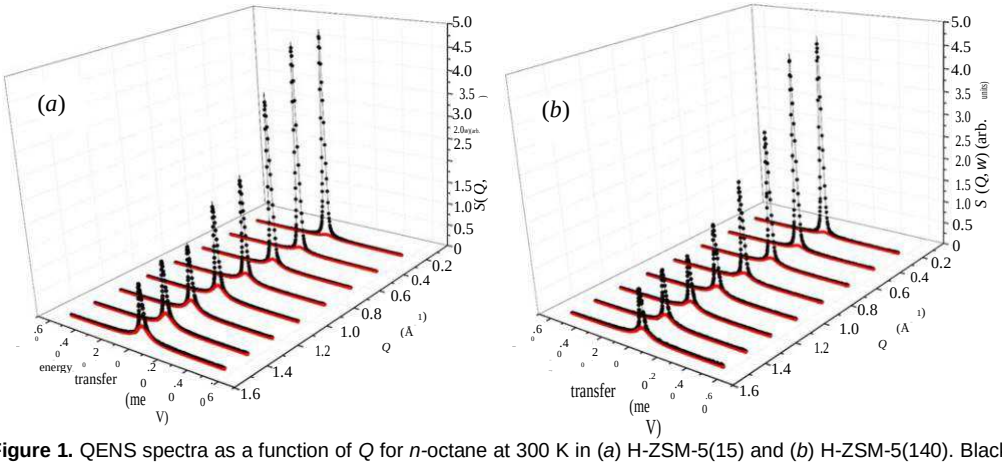

Figure 1. QENS spectra as a function of Q for *n*-octane at 300 K in (*a*) H-ZSM-5(15) and (*b*) H-ZSM-5(140). Black line is the total fit to the data points, red line is the quasi-elastic Lorentzian component. (Online version in colour.)

where $j1$ is the spherical Bessel function of the first kind. The model of 3-site jump rotation around a circle was also employed to represent an octane molecule where only the methyl groups are rotating, given by equation (3.3) (and shown by the red arrows in figure 3).

$$A_0(Q) = \frac{1}{3}\left(1 + 2j_0\left(Qr\sqrt{3}\right)\right), \tag{3.3}$$

where $j0$ is the 0th order Bessel function and r in this case is 1.04 Å representing the radius of the circle for the protons of a methyl group, shown by the red arrows in figure 3. The model of uniaxial rotation [29] was employed in our recent work to describe the rotation of oligomerized 1-octene around its long axis (shown by the black arrows in figure 3). The radius of rotation (r_u) of each octane proton around this long axis (derived in [28]) is calculated as 1.40 Å (though we note there may be slight deviations from this depending on the behaviour of the terminal methyl groups). This model cannot be used for powder samples typical in porous material studies, because no expression is available for the average angle θ between the axis of rotation and the direction of Q. However, one may consider a jump rotation over N sites around a circle similar to the 3-site model discussed earlier. With a sufficiently large N (greater than 6), the scattering function does not change as N increases, so the approximation of jump rotation over N sites may then be used as an approximate model for the EISF of continuous rotation, as given in equation (3.4)

$$A_0(Q) = \frac{1}{N}\sum_{n=1}^{N} j_0\left(2Qr_u \sin\frac{n\pi}{N}\right). \tag{3.4}$$

When the model of methyl rotation is used in isolation, it falls above the experimental points at all Q values (this is partially because when using this model, 2/3 of the protons must be considered static, which lifts the model line as detailed later). The model of diffusion confined to a sphere matching the ZSM-5 pore diameter falls below the experimental points at all but one Q value. We observe that the model of uniaxial rotation has a similar shape to the experimental data. We now consider the model EISFs, but with a mobile fraction fitted to take into consideration molecules which are unable to move on the timescale of the instrument, either due to interactions with the catalyst active sites or steric hindrance in the constrictive H-ZSM-5 channels, which is calculated as

$$A_{0\_\mathrm{eff}}(Q) = p_X A_0(Q) + (1 - p_X), \tag{3.5}$$

where p_X is the fraction of mobile molecules.

The optimal fits are shown in figure 4. The best fitting model is that of uniaxial rotation (with 17% of the protons treated as immobile) suggesting that the same mode of motion previously

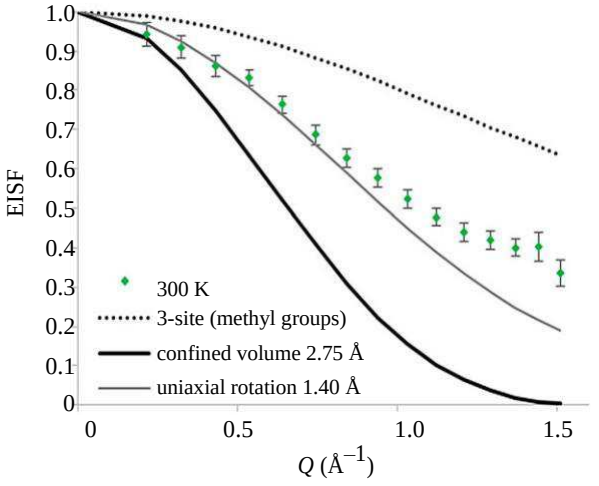

Figure 2. Experimental EISF plots of *n*-octane in H-ZSM-5(15) at 300 K against different theoretical EISF models. (Online version in colour.)

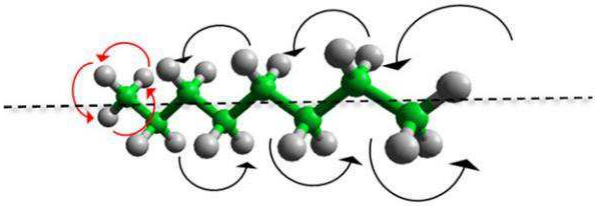

Figure 3. Schematic of an *n*-octane molecule illustrating the methyl rotational motion (red arrows) and the uniaxial rotation of protons around the dashed long axis. (Online version in colour.)

reported for oligomeric 1-octene is present for *n*-octane, despite the increase in degrees of freedom allowed for the single octane molecule. The error in this fitting is calculated by finding the best fit to the highest and lowest points on the error bars, giving an error of ±2.8%. This model of motion fits to the higher temperatures in H-ZSM-5(15) as shown in figure 4*a* with lower immobile populations (12 and 7% at 360 and 400 K, respectively), and also for all the experimental EISFs in H-ZSM-5(140) with immobile fractions of 11, 6 and 2% at 300, 360 and 400 K, respectively (the errors in these values are shown in table 1). We note that the immobile populations are consistently lower in the H-ZSM-5 catalyst with fewer Brønsted sites, suggesting the far lower prevalence or sorbate-acid site interactions allows for more molecules to undergo full-molecule uniaxial rotation in the channels. However, we note that the error bars for each fit to the EISF plots may signify that this difference in immobile populations may be smaller and the gap in population size should be treated with caution (figure 5).

The width of the quasi-elastic broadening in the measured neutron spectra is related to the rates of rotation. With rotational motions such as these, the quasi-elastic broadening will be independent of Q, as shown in figure 6*a*,*b*, where the half-width at half-maxima (HWHM, Γ) of the Lorentzian component fitted to the QENS spectra as a function of Q, are plotted for all temperatures of *n*-octane in H-ZSM-5(15) and H-ZSM-5(140), respectively. The broadenings show no Q-dependence, supporting the characterization of rotational motions, and increase in width with temperature suggesting an increase in rotational rate as would be expected. We note the widths are larger in ZSM-5(140) suggesting that in this sample not only are more molecules free to rotate, but those that are free also rotate faster in the sample with fewer acid sites.

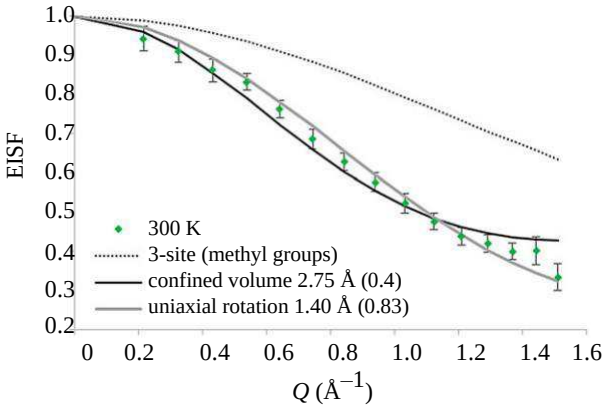

Figure 4. The experimental EISF of *n*-octane in H-ZSM-5(15) at 300 K, plotted against the models of localized motions after fitting with an immobile fraction. The optimump_X value is listed in brackets. (Online version in colour.)

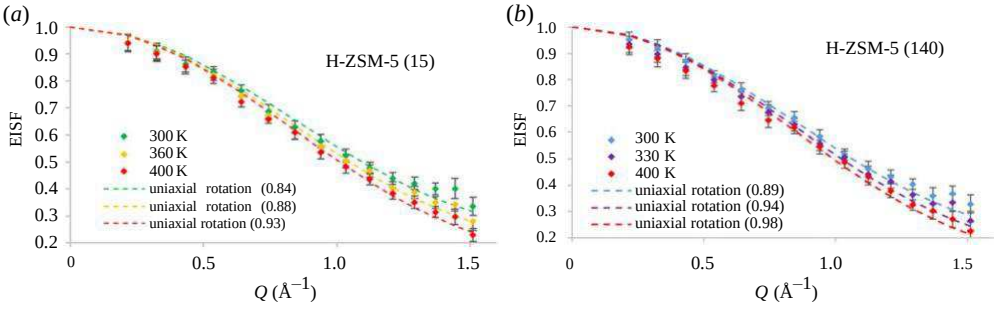

Figure 5. Experimental EISF of *n*-octane in H-ZSM-5(15) (*a*) and (140) (*b*) with the fitted uniaxial rotation model (optimal mobile fractions (p_X) shown in the legend in brackets). (Online version in colour.)

Table 1. Rotational diffusion coefficientsD_r) and mobile fractions of *n*-octane in H-ZSM-5(15) and (140).

	H-ZSM-5(15)		H-ZSM-5(140)	
T K	D_r s^{-1}	mobile fraction	D_r s^{-1}	mobile fraction
300	$7.4 \times 10^{10} \pm 0.25 \times 10^{10}$	0.84 ± 0.023	$8.1 \times 10^{10} \pm 0.27 \times 10^{10}$	0.89 ± 0.021
330	$7.8 \times 10^{10} \pm 0.29 \times 10^{10}$	0.88 ± 0.027	$8.5 \times 10^{10} \pm 0.28 \times 10^{10}$	0.94 ± 0.027
360	$8.5 \times 10^{10} \pm 0.32 \times 10^{10}$	0.93 ± 0.031	$9.1 \times 10^{10} \pm 0.30 \times 10^{10}$	0.98 ± 0.03
E_a (kJ mol^{-1})	4		3.3	

A model which approximates uniaxial rotation to a jump model of six sites around a circle (similar to that employed in modelling the EISF) which was used and detailed by Jobic *et al*. [29] to describe ethane, propane and other alkanes up to hexane [38] relates the Lorentzian HWHM to the jump rotation as

$$\Gamma = \frac{2}{\tau} \sin^2 \frac{\pi m}{6}, \qquad (3.6)$$

where τ is the mean time between successive rotational jumps (m is the order of the quasi-elastic structure factor), and the HWHM value at low Q may be used to calculate the rotational diffusion constant D_r as $1/2\tau$ as detailed in [29].

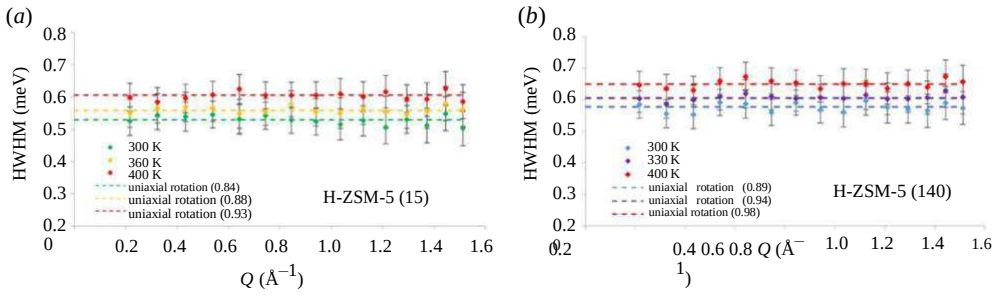

Figure 6. *Q*-dependence of the HWHM (Γ) of the quasi-elastic components of QENS spectra of *n*-octane in each H-ZSM-5 sample from 300 to 400 K. (Online version in colour.)

The calculated rotational diffusion coefficients (and mobile fractions) are shown in table 1, ranging from 7.4 to 8.5 × 10^{10} s^{-1} in H-ZSM-5(15) and 8.1–9.1 × 10^{-10} s^{-1} in H-ZSM-5(140), which along with the lower activation energy for rotation, illustrates the increased rotational freedom in ZSM-5(140). The D_r values are significantly higher (by about 30%) than those obtained for oligomerized 1-octene in H-ZSM-5 with a Si/Al = 30 [28]. This is not particularly surprising as the oligomerized chains (approx. C_{90}) are far less mobile than the C_8 monomer analogues in this study, further illustrated by the increase in the mobile population of octane molecules from 29% for oligomerized 1-octene to approximately 88% for *n*-octane at 330 K. The size of the increase in D_r at each temperature between H-ZSM-5(15) and (140) should be treated with caution when the experimental errors are considered. We note that the D_r values are approximately a factor of 5 lower than those calculated for the uniaxial rotation of propane in Na-ZSM-5, even though the loadings are double in terms of carbon atoms per unit cell and the Na^+ ion is present, illustrating the hindering effect of chain length on rotational motion.

(b) 2,5-dimethylhexane Dynamics

We now discuss the dynamics of 2,5-dimethylhexane in the H-ZSM-5 catalysts. QENS spectra as a function of *Q* for 2,5-dimethylhexane in H-ZSM-5(15) and (140) are shown in figures 7*a* and *b*, respectively. As with *n*-octane, the spectra were fit to the resolution function, a single Lorentzian function and a flat background function (apart from the lowest 2 *Q* groups in H-ZSM-5(15) where only a flat background was necessary, since there was no appreciable Lorentzian component). Upon visual comparison of figures 1 and 6, it is clear that the elastic components are more intense at high *Q* and the quasi-elastic components are lower in intensity than for *n*-octane in both samples. In addition, no quasi-elastic broadening is observed for the lowest 2 groups in H-ZSM-5(15), suggesting that no motions are observed at this *Q* range within the time window of the instrument (1–100 ps), so clearly the movement is very restricted.

The experimental EISF for 2,5-dimethylhexane in H-ZSM-5(15) at 300 K is shown in figure 8 along with relevant theoretical models, with a mobile fraction considered as for *n*-octane. We have applied the models of methyl rotation, and diffusion confined to a spherical volume with a diameter matching the ZSM-5 channels. We have also introduced a new model which incorporates the average radius of proton rotation around the long axis passing through a 2,5-dimethylhexane molecule centre of mass. The radius (1.75 Å for a 2,5-dimethylhexane molecule geometry optimized using the OPLS [39] forcefield) is feasible for rotation in the ZSM-5 channels and is depicted in figure 9.

Perhaps unsurprisingly–given the lack of any translational mobility observed for branched alkanes in previous QENS studies in ZSM-5 [27]—the model of confined translation diffusion is not able to fit the data, falling below the experimental points at low *Q* and above at high Q. The uniaxial rotation model is able to fit the datapoints within error at high Q, but falls below the points at low *Q*. The 3-site jump rotation model provides the best fit to the data. We note that

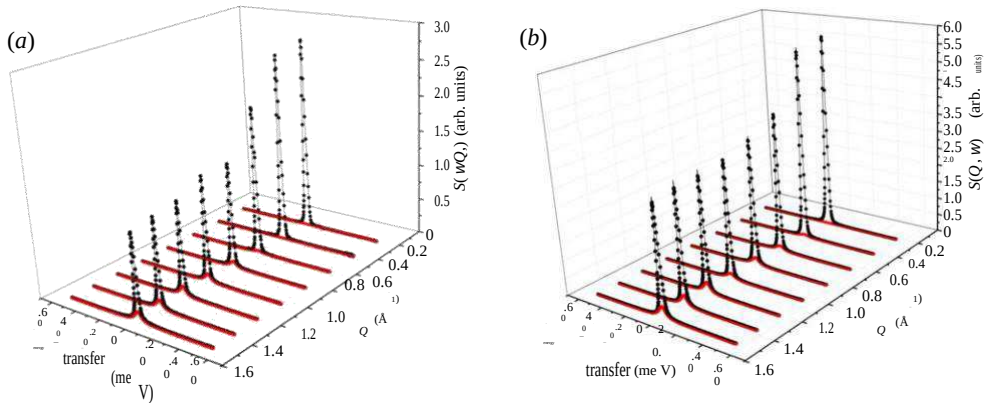

Figure 7. QENS spectra as a function of *Q* for 2,5-dimethylhexane at 300 K in zeolite (*a*) H-ZSM-5(15) and (*b*) H-ZSM-5(140). Black line is the total fit to the data points, red line is the quasi-elastic Lorentzian component. (Online version in colour.)

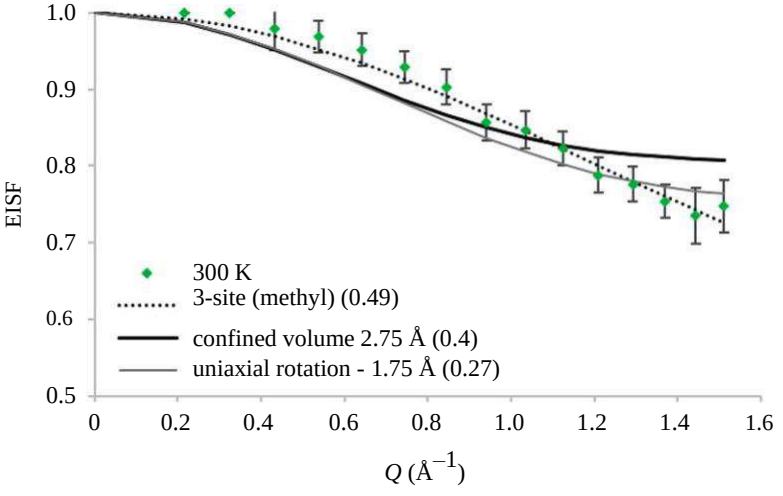

Figure 8. The experimental EISF of 2,5-dimethylhexane in H-ZSM-5(15) at 300 K, plotted against the models of localized motions after fitting with a mobile fraction. The optimump_X value is listed in brackets. (Online version in colour.)

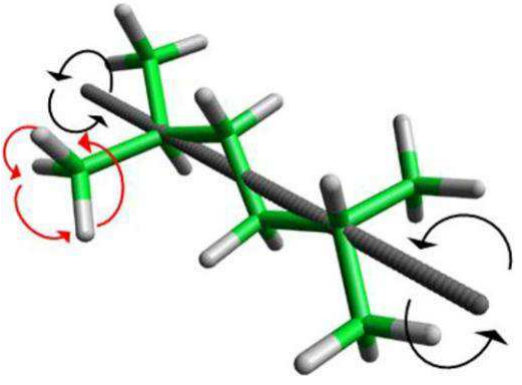

Figure 9. Schematic of an 2,5-dimethylhexane molecule illustrating the methyl rotational motion (red arrows) and the full molecule uniaxial rotation of protons around the dark grey long axis. (Online version in colour.)

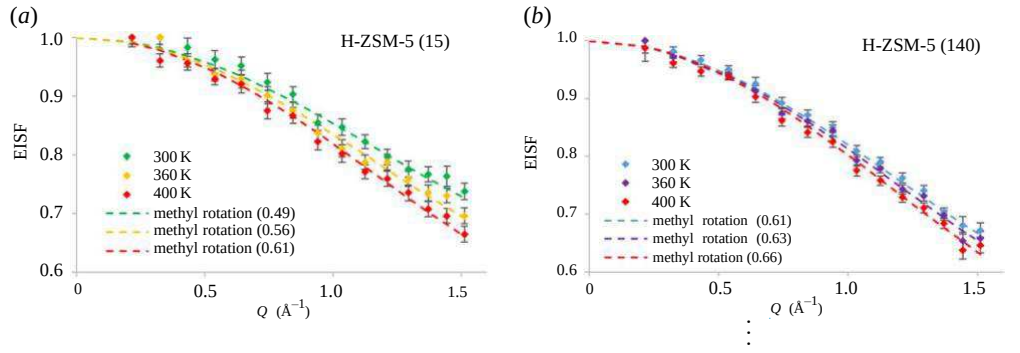

Figure 10. Experimental EISF of 2,5-dimethylhexane in (*a*) H-ZSM-5(15) and (*b*) (140) with the fitted 3-site jump rotation model for methyl rotation (optimal p_X shown in the legend in brackets). (Online version in colour.)

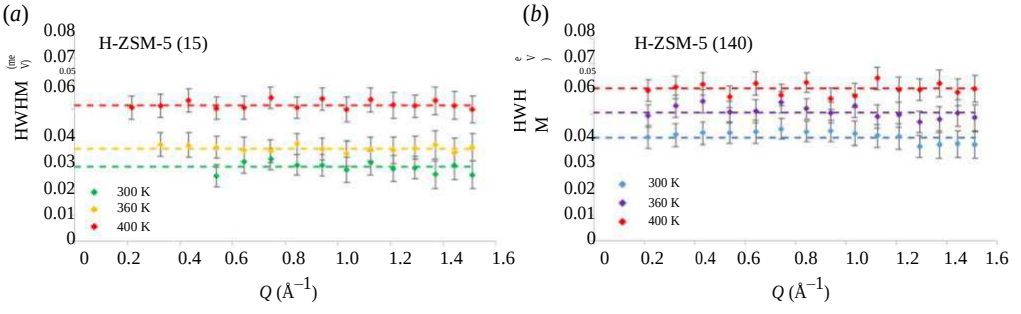

Figure 11. (*a–b*) *Q*-dependence of the HWHM (Γ) of the quasi-elastic components of QENS spectra of 2,5-dimethylhexane in each H-ZSM-5 sample from 300 to 400 K. (Online version in colour.)

the highest mobile fraction allowed for this model is 2/3, as this would encompass all the methyl protons in the molecule rotating. The mobile fraction at this temperature is 0.49, suggesting that in this sample, and at this temperature, movement is so restricted that not even all the methyl protons are able to rotate in the channels. The model EISF fits the data points for all temperatures in both samples as shown in figure 10*a*,*b*.

In H-ZSM-5(15), we note that the mobile fraction of methyl protons increases from 0.49 to 0.61 between 300 and 400 K, whereas in H-ZSM-5(140) the mobile fraction ranges from 0.61 to 0.66. Despite the whole molecule being immobile in terms of both translation and full molecule rotation, we observe that the lower concentration of Brønsted sites in ZSM-5 allows for more of the methyl groups in the system to rotate, illustrating that interactions with the acid sites can have a hindering effect even on intramolecular motions. However, we must note that the error bars on the EISF data points are large enough to overlap between datapoints recorded at intervals of 30 K—so conclusions in terms of mobile fractions must be drawn with caution, though the change in measured EISF is consistent with temperature and sample.

As with *n*-octane we may derive information on the rates of rotation from the widths of the Lorentzian component of the QENS spectra which are plotted in figure 11.

For a model of jump rotation over three equally spaced sites around a circle (assuming the probability of each site occupation is equal) the Lorentzian component of the scattering function is given by

$$L(\omega) = \frac{2\tau/3}{1+\omega^2(2\tau/3)^2} = \frac{\Gamma}{\Gamma^2+\omega^2}, \tag{3.7}$$

where the HWHM Γ is given by $3/2\tau$ and τ is the average time between consecutive jumps. One may calculate the activation energy (the potential barrier hindering rotation) using the Arrhenius Law. The residence times and activation energies are shown in table 2, with residence times ranging from 16.5 ps to 19 ps in H-ZSM-5(15) and 15.5 ps to 17.5 ps in H-ZSM-5(140).

Table 2. Time between mean jumps (τ) and mobile fractions and activation energies of methyl jump rotation of 2,5-dimethylhexane in H-ZSM-5(15) and (140).

	H-ZSM-5(15)		H-ZSM-5(140)	
T K	$\sim \tau$ s	mobile fraction	$\sim \tau$ s	mobile fraction
300	19 ± 0.57	0.49 ± 0.023	17.5 ± 0.55	0.61 ± 0.021
330	18 ± 0.54	0.56 ± 0.027	16.5 ± 0.51	0.63 ± 0.027
360	16.5 ± 0.55	0.61 ± 0.031	15.5 ± 0.53	0.66 ± 0.03
E_a (kJ mol^{-1})	4		3.5	

The activation energy for methyl jumps is only lower by 0.5 kJ mol^{-1} in H-ZSM-5(140), suggesting that acidic sites are less significant in the hindering of dimethylhexane methyl rotation than they are in the uniaxial rotation of *n*-octane, and the relatively long residence times are a product of steric hindrance from the constrictive ZSM-5 channels.

(c) On the local motions of hydrocarbons in H-ZSM-5 over the QENS timescale

The introduction of H-ZSM-5 as an additive catalyst to increase the yield of propene [40,41] (less than 5% product yield in typical FCC cracking catalysts [1]) is based on its much narrower pore system compared to the conventional catalysts based on zeolite Y (approx. 5.5 Å intersecting channels in ZSM-5, compared to the roughly spherical 13 Å supercages linked by 7.5 Å windows in zeolite Y). These narrower channels do not allow for bimolecular cracking mechanisms which involve bulkier transition states, or hydrogen transfer reactions. It is this steric constriction and the resulting imposed dynamical restrictions which were the focus of this study, particularly as we expect significant contrast between straight chain and branched isomers, in terms of mobility over the 10^{-11} to 10^{-9} s timescale probed by QENS instruments. Within this timescale are a range of molecular motions including translational diffusion through the framework structure [42,43], local/confined diffusion [44], full-molecule rotations [45] and intramolecular rotations. Translational diffusion of *n*-octane was probed in ZSM-5 by Jobic *et al*. [27], obtaining diffusion coefficients in the region of 10^{-10} to 10^{-11} m^2 s^{-1} using the high resolution backscattering spectrometer IN16 at ILL Grenoble, where the μeV resolution (observing motions in the time window of 0.2–10 ns) allows for the slow diffusive processes in this system to be probed. However, they were not able to determine the diffusivity of a branched alkane (in this case isobutane) as it was too slow even for the higher resolution backscattering spectrometers. Later studies have shown that in the MFI zeolite topology upon which the ZSM-5 is based, the neutron spin-echo technique (which is able to probe motion over the timescale of approx. 100 ns [24]), can measure diffusivities of such branched species as low as 1×10^{-11} m^2 s^{-1} at 444 K [19]. However, it should be noted that this is in the fully siliceous MFI system (silicalite-1) without acidic sites/counterions for the sorbate to bind to, which slows diffusion significantly.

It is clear that if one aims to directly compare the motion of straight chain and branched isomers (particularly larger C_8 species) using one instrument, we are limited to more local motions such as rotations, and locally confined translational motions which take place over the faster (ps) timescales where even an order of magnitude difference may be observed in the approximately 1–100 ps window observed by a backscattering spectrometer with an energy resolution on the order of 10 μeV. Examples of such rotational studies include the uniaxial rotation of ethane and propane in Na-ZSM-5, where ethane gave D_r values of 1–2 × 10^{11} s^{-1} (propane was similar at 300 K) which is roughly a factor of 2 higher that the uniaxial D_r calculated for octane in this study. One might consider that the difference in rates of motion between ethane/propane and octane in this similar system would be far greater. However, it is important to consider that Na-ZSM-5 possesses a far larger and more strongly adsorbing counterion than the Brønsted acid sites involved in this study, which would likely hinder rotational motion more. A mobile/immobile

fraction of molecules is not reported either, and if all the molecules are able to rotate then this system is displaying a far greater degree of rotational freedom than our octane in H-ZSM-5 system as expected. Studies of more bulky molecules in H-ZSM-5 include xylene [46], where the uniaxial methyl rotation of only one of the two xylene methyl groups was observed, while the other methyl group was said to be interacting strongly with the channel walls, but no D_r values were reported for comparison with our dimethylhexane values. However, it is worth noting that the authors gained a great deal of insight from the comparison with structural studies and simulations to show how both the orientation and location of *m*- and *p*- xylene isomers lead to this methyl rotation blocking. Cyclohexane rotation in H-ZSM-5 has also been studied [47] and through the fitting of a 3-site jump rotation model it was concluded that cyclohexane was in the chair conformation, the D_{3d} symmetry of which would allow for such rotations to be observed with a residence time of 8.2 ps at room temperature. We note that this is roughly twice as fast as that found for our methyl groups in dimehylhexane which, given the size of the cyclohexane molecule/circle around which the protons are jumping, may seem strange. However, we must consider that molecules of similar dimensions such as benzene tend to locate at the channel intersections in ZSM-5, where isotropic and sixfold rotations may be observed [48,49]. Given the much larger void volume of the MFI channel intersections compared to the channels (where we expect our dimethylhexane molecules to be sited if the only motions observable are methyl rotations), the extra freedom of rotation in the larger cyclohexane molecule may not be an unreasonable observation.

It is clear from the referenced studies that probing local motions of hydrocarbons in cracking catalysts can yield some very insightful observations in terms of molecular behaviour and interactions, necessary for catalyst optimization. In the absence of clear vibrational spectroscopic features at the relevant temperatures to illustrate any strong interactions between the catalyst active sites and aliphatic hydrocarbons, such rotational dynamical data may prove a key descriptor for strong interactions with the walls of the catalyst micropores. The value of such local motions in the field of microporous catalysis (certainly in terms of their input into typical kinetic models, where a more standard translational diffusion coefficient is commonplace) is yet to be realized, and future QENS/NSE experiments will focus on building a complete picture of the dynamical behaviour across scales in addition to these observations.

4. Summary and conclusions

The dynamical behaviour of *n*-octane and 2,5-dimethylhexane was probed in two H-ZSM-5 samples with Si/Al = 15 and 140 using quasi-elastic neutron scattering, to study the effect of molecular shape and Brønsted acid site density on the dynamics of common FCC species in acidic zeolite catalysts, where H-ZSM-5 is an additive catalyst. Translational diffusion was not observed on the 1–100 ps timescale of the QENS instrument. However, for *n*-octane, the EISF could be fit to the model of uniaxial rotation along its long axis with rotational diffusion coefficients in the range of 7.5 to 8.5 × 10^{10} s^{-1} (with a mobile population between 84 and 93%) in ZSM-5(15), and 8.1 to 9.1 × 10^{10} s^{-1} (with a mobile population between 89 and 98%) in ZSM-5(140). The higher rotational constants and larger mobile populations in H-ZSM-5(140) compared to H-ZSM-5(15) suggest that the much lower concentration of Brønsted acid sites in H-ZSM-5(140) allows for freer rotation of *n*-octane in the ZSM-5 channels. 2,5-dimethylhexane is probably too bulky to rotate fully in the ZSM-5 channels, as the only dynamics which could be observed were the rotations of its methyl groups. The residence times between jumps ranged between 16.5 and 19 ps (with a mobile population of between 49 and 61%) in H-ZSM-5(15) and between 15.5 and 17.5 ps (with a mobile population of 49–61%) in H-ZSM-5(140). The long residence times reflect the steric hindrance exerted by the ZSM-5 channels, while the (slight) decrease in residence times measured in H-ZSM-5(140) compared to H-ZSM-5(15) may reflect less of a hindrance to methyl rotations with fewer Brønsted acid sites present. The study highlights the effect of molecular shape and branching on the qualitative difference in behaviour of the isomers in H-ZSM-5, while also showing the effect that a difference in Si/Al ratio (and thus acid site density) can have on the

quantitative rates of motion, and the number of immobile molecules/moieties inside this zeolite catalyst.

Data accessibility. The data used in this paper was from the ISIS Neutron and Muon source (experiment RB1220109 and RB1310046) and as such may be accessed from https://data.isis.stfc.ac.uk

Authors' contributions. Experiments carried out or facilitated by A.J.O.M., N.D., W.J., S.F.P. and V.G.S. Analysis carried out by A.J.O.M. and V.G.S. All aspects of the study carried out by AJOM were carried out under the supervision of CRAC. All authors have contributed to the manuscript. All authors have read and approved the manuscript.

Competing interests. The authors declare that they have no competing interest.

Funding. We acknowledge the Engineering and Physical Sciences Research Council (EPSRC): grant no. EP/G036675/1 for financial support under their Centres for Doctoral Training scheme and the Science and Technologies Facilities Council. The UK Catalysis Hub is kindly thanked for resources and support provided via our membership of the UK Catalysis Hub Consortium and funded by EPSRC (grant nos EP/K014706/1, EP/K014668/1, EP/K014854/1EP/K014714/1 and EP/M013219/1). The data upon which this paper is based may be accessed from the ISIS Data Catalogue (https://data.isis.stfc.ac.uk/) using the RB numbers specified above.

Acknowledgements. A.J.O.M. acknowledges Roger and Sue Whorrod for the funding of the Whorrod Fellowship. The STFC Rutherford Appleton Laboratory/ISIS Pulsed Neutron and Muon Source is thanked for access to neutron beam facilities (experiment RB1220109 and RB1310046) and for funding and sponsorship of A.J.O.M.

References

1. Vogt ETC, Weckhuysen BM. 2015 Fluid catalytic cracking: recent developments on the grand old lady of zeolite catalysis. *Chem. Soc. Rev.* **44**, 7342–7370. (doi:10.1039/C5CS00376H)
2. Scherzer J. 1989 Octane-enhancing, zeolitic FCC catalysts: scientific and technical aspects. *Catalysis Reviews - Science and Engineering* **31**, 215–354.
3. Venuto PB, Habib ETJ. 1979 Fluid catalytic cracking with zeolite catalysts.
4. Al-Sabawi M, Chen J, Ng S. 2012 Fluid catalytic cracking of biomass-derived oils and their blends with petroleum feedstocks: a review. *Energy Fuels* **26**, 5355–5372. (doi:10.1021/ef3006417)
5. Corma A, Huber GW, Sauvanaud L, O'Connor P. 2007 Processing biomass-derived oxygenates in the oil refinery: catalytic cracking (FCC) reaction pathways and role of catalyst. *J. Catal.* **247**, 307–327. (doi:10.1016/j.jcat.2007.01.023)
6. Arandes JM, Abajo I, López-Valerio D, Fernández I, Azkoiti MJ, Olazar M, Bilbao J. 1997 Transformation of several plastic wastes into fuels by catalytic cracking. *Ind. Eng. Chem. Res.* **36**, 4523–4529. (doi:10.1021/ie970096e)
7. Smit B, Maesen TLM. 2008 Towards a molecular understanding of shape selectivity. *Nature* **451**, 671–678. (doi:10.1038/nature06552)
8. Chen NY, Degnan Jr TF, Smith CM. 1994 *Molecular transport and reaction in zeolites: design and application of shape selective catalysis*. New York, NY: John Wiley & Sons.
9. Jiang M, Eic M, Miachon S, Dalmon J-A, Kocirik M. 2001 Diffusion of n-butane, isobutane and ethane in a MFI-zeolite membrane investigated by gas permeation and ZLC measurements. *Sep. Purif. Technol.* **25**, 287–295. (doi:10.1016/S1383-5866(01)00055-7)
10. Leroy F, Rousseau B. 2004 Self-diffusion of n-alkanes in MFI type zeolite using molecular dynamics simulations with an anisotropic united atom (AUA) forcefield. *Mol. Simul.* **30**, 617– 620. (doi:10.1080/08927020410001717272)
11. Krishna R, van Baten JM. 2008 Diffusion of hydrocarbon mixtures in MFI zeolite: influence of intersection blocking. *Chem. Eng. J.* **140**, 614–620. (doi:10.1016/j.cej.2007.11.026)
12. Koriabkina AO, de Jong AM, Schuring D, van Grondelle J, van Santen RA. 2002 Influence of the acid sites on the intracrystalline diffusion of hexanes and their mixtures within MFI-zeolites. *J. Phys. Chem. B* **106**, 9559–9566. (doi:10.1021/jp014464a)
13. Yu M, Wyss JC, Noble RD, Falconer JL. 2008 2,2-Dimethylbutane adsorption and diffusion in MFI zeolite. *Microporous Mesoporous Mater.* **111**, 24–31. (doi:10.1016/j.micromeso.2007.07.001)
14. Fried JR, Weaver S. 1998 Atomistic simulation of hydrocarbon diffusion in silicalite. *Comput. Mater. Sci.* **11**, 277–293. (doi:10.1016/S0927-0256(98)00012-3)

15. Jianfen F, van de Graaf B, Xiao HM, Njo SL. 1999 Molecular dynamics simulation of ethene diffusion in MFI and H[Al]ZSM-5. *J. Mol. Struct. THEOCHEM* **492**, 133–142. (doi:10.1016/S0166-1280(99)00158-X)
16. Millot B, Méthivier A, Jobic H, Moueddeb H, Bée M. 1999 Diffusion of isobutane in ZSM-5 zeolite: a comparison of quasi-elastic neutron scattering and supported membrane results. *J. Phys. Chem. B* **103**, 1096–1101. (doi:10.1021/jp982897g)
17. O'Malley AJ, Catlow CRA. 2013 Molecular dynamics simulations of longer n-alkanes in silicalite: a comparison of framework and hydrocarbon models. *Phys. Chem. Chem. Phys.* **15**, 19 024–19 030. (doi:10.1039/C3CP52653D)
18. O'Malley AJ, Catlow CR. 2015 Molecular dynamics simulations of longer n-alkanes in silicalite: state-of-the-art models achieving close agreement with experiment. *Phys. Chem. Chem. Phys.* **17**, 1943–1948. (doi:10.1039/C4CP04898A)
19. O'Malley AJ, Catlow CRA, Monkenbusch M, Jobic H. 2015 Diffusion of Isobutane in Silicalite: a neutron spin–echo and molecular dynamics simulation study. *J. Phys. Chem. C* **119**, 26 999– 27 006. (doi:10.1021/acs.jpcc.5b08048)
20. O'Malley AJ, Parker SF, Catlow CRA. 2017 Neutron spectroscopy as a tool in catalytic science. *Chem. Commun.* **53**, 12 164–12 176. (doi:10.1039/C7CC05982E)
21. Jacobs WPJH, Jobic H, van Wolput JHMC, van Santen RA. 1992 Fourier transform infrared and inelastic neutron scattering study of HY zeolites. *Zeolites* **12**, 315–319. (doi:10.1016/ S0144-2449(05)80301-X)
22. Potter ME, Chapman S, O'Malley AJ, Levy A, Carravetta M, Mezza TM, Parker SF, Raja R. 2017 Understanding the role of designed solid acid sites in the low-temperature production of ***ε***-Caprolactam. *ChemCatChem* **9**, 1897–1900. (doi:10.1002/cctc.201700516)
23. Jobic H. 2002 Neutron scattering methods for the study of zeolites. *Curr. Opin. Solid State Mater. Sci.* **6**, 415–422. (doi:10.1016/S1359-0286(02)00111-0)
24. Jobic H, Theodorou DN. 2007 Quasi-elastic neutron scattering and molecular dynamics simulation as complementary techniques for studying diffusion in zeolites. *Microporous Mesoporous Mater.* **102**, 21–50. (doi:10.1016/j.micromeso.2006.12.034)
25. Jobic H, Schmidt W, Krause CB, Kärger J. 2006 PFG NMR and QENS diffusion study of n-alkane homologues in MFI-type zeolites. *Microporous Mesoporous Mater.* **90**, 299–306. (doi:10.1016/j.micromeso.2005.10.020)
26. Jobic H, Theodorou DN. 2006 Diffusion of long n-alkanes in silicalite. A comparison between neutron scattering experiments and hierarchical simulation results. *J. Phys. Chem. B* **110**, 1964–1967. (doi:10.1021/jp056924w)
27. Jobic H. 2000 Diffusion of linear and branched alkanes in ZSM-5. A quasi-elastic neutron scattering study. *J. Mol. Catal. A: Chem.* **158**, 135–142. (doi:10.1016/S1381-1169(00)00057-1)
28. Hawkins AP, O'Malley AJ, Zachariou A, Collier P, Ewings RA, Silverwood IP, Howe RF, Parker SF, Lennon D. 2019 Investigation of the dynamics of 1-octene adsorption at 293 K in a ZSM-5 catalyst by inelastic and quasielastic neutron scattering. *J. Phys. Chem. C* **123**, 417–425. (doi:10.1021/acs.jpcc.8b08420)
29. Jobic H, Bée M, Kearley GJ. 1992 Dynamics of ethane and propane in zeolite ZSM-5 studied by quasi-elastic neutron scattering. *Zeolites* **12**, 146–151. (doi:10.1016/0144-2449(92)90075-Z)
30. Matam SK *et al.* 2018 The effects of MTG catalysis on methanol mobility in ZSM-5. *Catalysis Sci. Technol.* **8**, 3304–3312. (doi:10.1039/C8CY00422F)
31. Li M, Zhou Y, Oduro IN, Fang Y. 2016 Comparative study on the catalytic conversion of methanol and propanal over Ga/ZSM-5. *Fuel* **168**, 68–75. (doi:10.1016/j.fuel.2015.11.076)
32. Tarach KA, Martinez-Triguero J, Rey F, Góra-Marek K. 2016 Hydrothermal stability and catalytic performance of desilicated highly siliceous zeolites ZSM-5. *J. Catal.* **339**, 256–269. (doi:10.1016/j.jcat.2016.04.023)
33. Telling MTF, Andersen KH. 2005 Spectroscopic characteristics of the OSIRIS near-backscattering crystal analyser spectrometer on the ISIS pulsed neutron source. *Phys. Chem. Chem. Phys.* **7**, 1255–1261. (doi:10.1039/B413934H)
34. Azuah RT, Kneller LR, Qiu Y, Tregenna-Piggott PLW, Brown CM, Copley JRD, Dimeo RM. 2009 DAVE: a comprehensive software suite for the reduction, visualization, and analysis of low energy neutron spectroscopic data. *J. Res. Natl Inst. Stand. Technol.* **114**, 341–358. (doi:10.6028/jres.114.025)

35. Arnold O *et al.* 2014 Mantid—data analysis and visualization package for neutron scattering and μ SR experiments. Nuclear instruments and methods in physics research section a: accelerators, spectrometers, detectors and associated equipment **764**, 156–166. (doi:10.1016/j.nima.2014.07.029)

36. Bée M. 1988 *Quasielastic neutron scattering*. Bristol: Adam Hilger.
37. O'Malley AJ, Catlow CRA. 2017 Chapter 6 - Sorbate Dynamics in Zeolite Catalysts. In *Experimental methods in the physical sciences* (eds F Fernandez-Alonso, DL Price), pp. 349–401. New York, NY: Academic Press.
38. Jobic H, Bee M, Caro J. 1993 Translational mobility of n-butane and n-hexane in zsm-5 measured by quasi-elastic neutron scattering. In *Proceedings from the ninth international zeolite conference* (eds R von Ballmoos, JB Higgins, MMJ Treacy), pp. 121–128. Butterworth-Heinemann.

39. Jorgensen WL, Maxwell DS, Tirado-Rives J. 1996 Development and testing of the OPLS all-atom force field on conformational energetics and properties of organic liquids. *J. Am. Chem. Soc.* **118**, 11 225–11 236. (doi:10.1021/ja9621760)
40. Hydrocarbon Processing (2011), 90(9), 91–95 - google scholar. See https://scholar.google.co.uk/scholar?hl=en&as_sdt=0%2C5&q=Hydrocarbon+Processing+%282011%29%2C+90%289%29%2C+91-95&btnG (accessed 8 April 2020) (In press).
41. Degnan TF, Chitnis GK, Schipper PH. 2000 History of ZSM-5 fluid catalytic cracking additive development at Mobil. *Microporous Mesoporous Mater.* **35–36**, 245–252. (doi:10.1016/ S1387-1811(99)00225-5)
42. O'Malley AJ, Sakai VG, Silverwood IP, Dimitratos N, Parker SF, Catlow CRA. 2016 Methanol diffusion in zeolite HY: a combined quasielastic neutron scattering and molecular dynamics simulation study. *Phys. Chem. Chem. Phys.* **18**, 17 294–17 302. (doi:10.1039/C6CP01151A)
43. O'Malley AJ, Hitchcock I, Sarwar M, Silverwood IP, Hindocha S, Catlow CRA, York APE, Collier PJ. 2016 Ammonia mobility in chabazite: insight into the diffusion component of the NH 3 -SCR process. *Phys. Chem. Chem. Phys.* **18**, 17 159–17 168. (doi:10.1039/C6CP01160H)
44. O'Malley AJ, Sarwar M, Armstrong J, Catlow CR, Silverwood IP, York AP, Hitchcock I. 2018 Comparing ammonia diffusion in NH 3-SCR zeolite catalysts: a quasielastic neutron scattering and molecular dynamics simulation study. *Phys. Chem. Chem. Phys.* **20**, 11 976– 11 986. (doi:10.1039/C8CP01022F)
45. Hernandez-Tamargo C, O'Malley AJ, Silverwood IP, Leeuw NH de. 2019 Molecular behaviour of phenol in zeolite Beta catalysts as a function of acid site presence: a quasielastic neutron scattering and molecular dynamics simulation study. *Catal. Sci. Technol.* **9**, 6700–6713. (doi:10.1039/C9CY01548E)
46. Czjzek M, Jobic H, Bée M. 1991 Molecular dynamics of xylene in Na, Yb-Y and ZSM-5 studied by quasi-elastic neutron scattering. *J. Chem. Soc. Faraday Trans.* **87**, 3455–3459. (doi:10.1039/FT9918703455)
47. Sahasrabudhe A, Mitra S, Tripathi AK, Mukhopadhyay R, Gupta NM. 2003 Effect of pore characteristics on the dynamics of cyclohexane molecules confined in ZSM-5 and MCM-41 molecular sieves: FTIR and QENS study. *Phys. Chem. Chem. Phys.* **5**, 3066–3075. (doi:10.1039/B303782G)
48. Jobic H, Bée M, Dianoux AJ. 1989 Quasi-elastic neutron scattering study of benzene adsorbed in ZSM-5. *J. Chem. Soc. Faraday Trans.* **1** 85, 2525. (doi:10.1039/f19898502525)
49. Mitra S, Tripathy AK, Gupta NM, Mukhopadhyay R. 2002 Molecular motions of benzene adsorbed in ZSM-5 zeolite: quasielastic neutron scattering study. *Appl. Phys. A: Mater. Sci. Process.* **74**, s1308–s1310. (doi:10.1007/s003390201378)